

Uncovering the abilities of *Agaricus bisporus* to degrade plant biomass throughout its life cycle

Aleksandrina Patyshakuliyeva,¹ Harm Post,^{2,3}
Miaomiao Zhou,¹ Edita Jurak,⁴ Albert J. R. Heck,^{2,3}
Kristiina S. Hildén,⁵ Mirjam A. Kabel,⁴
Miia R. Mäkelä,⁵ Maarten A. F. Altelaar^{2,3} and
Ronald P. de Vries^{1*}

¹Fungal Physiology, CBS-KNAW Fungal Biodiversity Centre & Fungal Molecular Physiology and

²Biomolecular Mass Spectrometry and Proteomics, Bijvoet Centre for Biomolecular Research and Utrecht Institute for Pharmaceutical Sciences, Utrecht University, Padualaan 8, 3584 CH Utrecht, The Netherlands.

³Netherlands Proteomics Centre, Padualaan 8, 3584 CH Utrecht, The Netherlands.

⁴Laboratory of Food Chemistry, Wageningen University, Borse Weiland 9, 6708 WG, Wageningen, The Netherlands.

⁵Department of Food and Environmental Sciences, University of Helsinki, P. O. Box 56, 00014 Helsinki, Finland.

Summary

The economically important edible basidiomycete mushroom *Agaricus bisporus* thrives on decaying plant material in forests and grasslands of North America and Europe. It degrades forest litter and contributes to global carbon recycling, depolymerizing (hemi-)cellulose and lignin in plant biomass. Relatively little is known about how *A. bisporus* grows in the controlled environment in commercial production facilities and utilizes its substrate. Using transcriptomics and proteomics, we showed that changes in plant biomass degradation by *A. bisporus* occur throughout its life cycle. Ligninolytic genes were only highly expressed during the spawning stage day 16. In contrast, (hemi-)cellulolytic genes were highly expressed at the first flush, whereas low expression was observed at the second flush. The essential role for many highly expressed plant biomass degrading genes was supported by exoproteome analysis. Our data also support a model of

sequential lignocellulose degradation by wood-decaying fungi proposed in previous studies, concluding that lignin is degraded at the initial stage of growth in compost and is not modified after the spawning stage. The observed differences in gene expression involved in (hemi-)cellulose degradation between the first and second flushes could partially explain the reduction in the number of mushrooms during the second flush.

Introduction

Agaricus bisporus, commonly known as the button mushroom, is a saprotrophic secondary decomposing basidiomycete, mainly occupying ecological niches rich in lignocellulose such as leaf and forest litter, and grasslands, and thus has an important role in carbon recycling. In addition, *A. bisporus* is the most widely produced mushroom for human consumption in the world. Commercially, it is cultivated on a variety of organic substrates, such as wheat straw, and horse and chicken manure-based compost (Gerrits, 1988). Spawn (*A. bisporus* mycelium developed on cereal grain) is introduced into this composted mixture, and the fungus starts growing vegetatively while colonizing its substrate (Chang and Miles, 1989). During commercial cultivation, the switch from the vegetative to reproductive stage occurs when fully colonized compost is covered with a non-nutritious 'casing' layer (mainly peat and lime). Further distribution of mycelial cords in the casing layer and its aggregation forms primordia, which continue to develop into mature mushrooms. After a developed crop (flush) is harvested, new flushes appear in a rhythmic mode almost at weekly intervals (Van Griensven, 1988). This controlled environment also provides an ideal system to study the degradation of plant biomass during the different stages of a basidiomycete life cycle.

Despite the ecological and economic importance of button mushrooms, relatively little is known about how it degrades substrate throughout its life cycle. Several studies of the compost composition have shown that it consists mainly of cellulose, hemicellulose and lignin (Gerrits *et al.*, 1967; Iiyama *et al.*, 1994; Jurak *et al.*, 2014), with the major carbohydrate fraction represented by xylosyl and glucosyl residues (Jurak *et al.*, 2014). *Agaricus bisporus* grows well on compost, which correlates with its

Received 16 February, 2015; revised 18 June, 2015; accepted 20 June, 2015. *For correspondence. E-mail r.devries@cbs.knaw.nl; Tel. +31 (0)30 2122600; Fax (+31) 30 2512097.

potential to secrete large amounts of carbohydrate active enzymes (CAZy, <http://www.cazy.org>) (Lombard *et al.*, 2014) to degrade lignocellulose and use released constituents as the carbon source (Gerrits, 1969; Wood *et al.*, 1991; Yague *et al.*, 1997; Hilden *et al.*, 2013).

The complete genome sequence of *A. bisporus* (Morin *et al.*, 2012) facilitated the identification of a full repertoire of genes encoding CAZymes and showed that *A. bisporus* has adapted to the environment where lignocellulose, lignocellulosic-derived material and humic substances are present (Morin *et al.*, 2012). Using a transcriptomics approach of a single time point (the moment when the first flush of mushrooms was produced), recent studies demonstrated a predominant substrate preference for cellulose and xylan based on which genes were expressed during growth of *A. bisporus* on compost (Morin *et al.*, 2012) and the carbohydrate composition of compost (Patyshakuliyeva *et al.*, 2013). Also, there is a difference in the set of CAZyme-encoding genes expressed in compost grown mycelium and in fruiting bodies. Genes encoding plant cell wall degrading enzymes were expressed in vegetative mycelium grown in compost and largely absent in fruiting bodies (Patyshakuliyeva *et al.*, 2013). However, genes encoding fungal cell wall modifying enzymes were expressed in both samples, but the gene sets were different (Patyshakuliyeva *et al.*, 2013).

Thus far, the above-mentioned studies shed light on the lignocellulose-degrading capabilities of *A. bisporus*, its adaptation to humic-rich environment and importance for terrestrial carbon cycling. However, these studies provide mainly snapshots of the physiology of *A. bisporus* focusing mainly on a transcriptome analysis of only single time point (first flush). Therefore, the study presented here aims to gain a thorough understanding of the carbon nutritive needs of *A. bisporus* and its potential to degrade plant biomass at different stages of its life cycle using the controlled environment of indoor commercial cultivation. This study represents the first temporal transcriptome and secretome analysis of *A. bisporus* in compost as well as composition analysis of the substrate beginning with the vegetative mycelium associated with the spawning stage and ending with the growth stage when all second flush mushrooms were harvested.

Results

Transcriptome of various growth stages of A. bisporus grown in compost under commercial cultivation conditions

High throughput sequencing (RNA-seq) was performed to examine transcriptome of *A. bisporus* grown in compost and the gene expression at different growth stages. The RPKM method (reads per kilobase per million) (Mortazavi

et al., 2008) was used to determine the normalized mRNA abundance. RPKM values were calculated for each of the biological replicates. In this analysis RPKM 300 was taken as the threshold for highly expressed genes. A cut-off of fold change of ≥ 1.5 and *P*-value of < 0.05 was used to identify differentially expressed genes between all growth stages. The most significant expression difference up to 1000-folds was found when the growth stages were compared with the spawning stage day 16 (Table S1).

Expression of CAZy genes

CAZyme-encoding genes represented 3% (376 of 9620 genes) of the total *A. bisporus* genes identified in all growth stages, with genes from the glycoside hydrolase (GH) families representing approximately half (46%) of the total CAZy mRNA (Table S1). The CAZymes encoding genes from the auxiliary activities (AAs), the carbohydrate esterases (CEs) and the polysaccharide lyases (PLs) families represented 22%, 9% and 2%, respectively, of the total CAZy mRNA (Table S1).

Among all the growth stages of *A. bisporus* in compost, transcripts predicted to encode cellulose-degrading enzymes were generally the most abundant ones (Fig. 1, Table S1). On average, expression of the genes that are involved in degradation of cellulose slightly increased over time from the spawning stage day 16 until the first flush (Table S1). After all the first flush mushrooms were harvested, expression of the genes dropped and then again increased after all the second flush mushrooms were harvested. Exceptions to this profile included one out of six AA9 lytic polysaccharide monoxygenase (Gene ID 196143) encoding genes, which showed the highest expression during spawning stage day 16 (Fig. 1, Table S1). A similar expression profile was observed for genes involved in hemicellulose degradation (Table S1). Highly expressed cellulolytic genes were found during the first flush and during the growth stage when all second flush mushrooms were harvested as compared with the other growth stages. These genes reached an expression level above 300 RPKM and include 6 AA9 lytic polysaccharide monoxygenases, 3 GH5_5 and 1 GH12 endoglucanase, 1 GH1 β -glucosidase, and 1 GH6 and 1 GH7 cellobiohydrolase (Fig. 1).

Similar to the expression of cellulolytic genes, transcripts predicted to encode hemicellulose-degrading enzymes were most abundant during the first flush and during the growth stage when all second flush mushrooms were harvested and had comparatively low abundance during the other stages of *A. bisporus* growth in compost (Fig. 1, Table S1). Hemicellulolytic genes with RPKM values above 300 are represented by 1 GH10 and 2 GH11 endoxylanases, 1 GH27 α -galactosidase, 1 GH35 β -galactosidase, 1 GH5_22 β -xylosidase, 1 GH51



Fig. 1. Visualization of the RNA expression levels, carbohydrate and lignin contents across the growth of *A. bisporus* in compost. *Sum of arabinosyl, xylosyl, glucuronic acid.

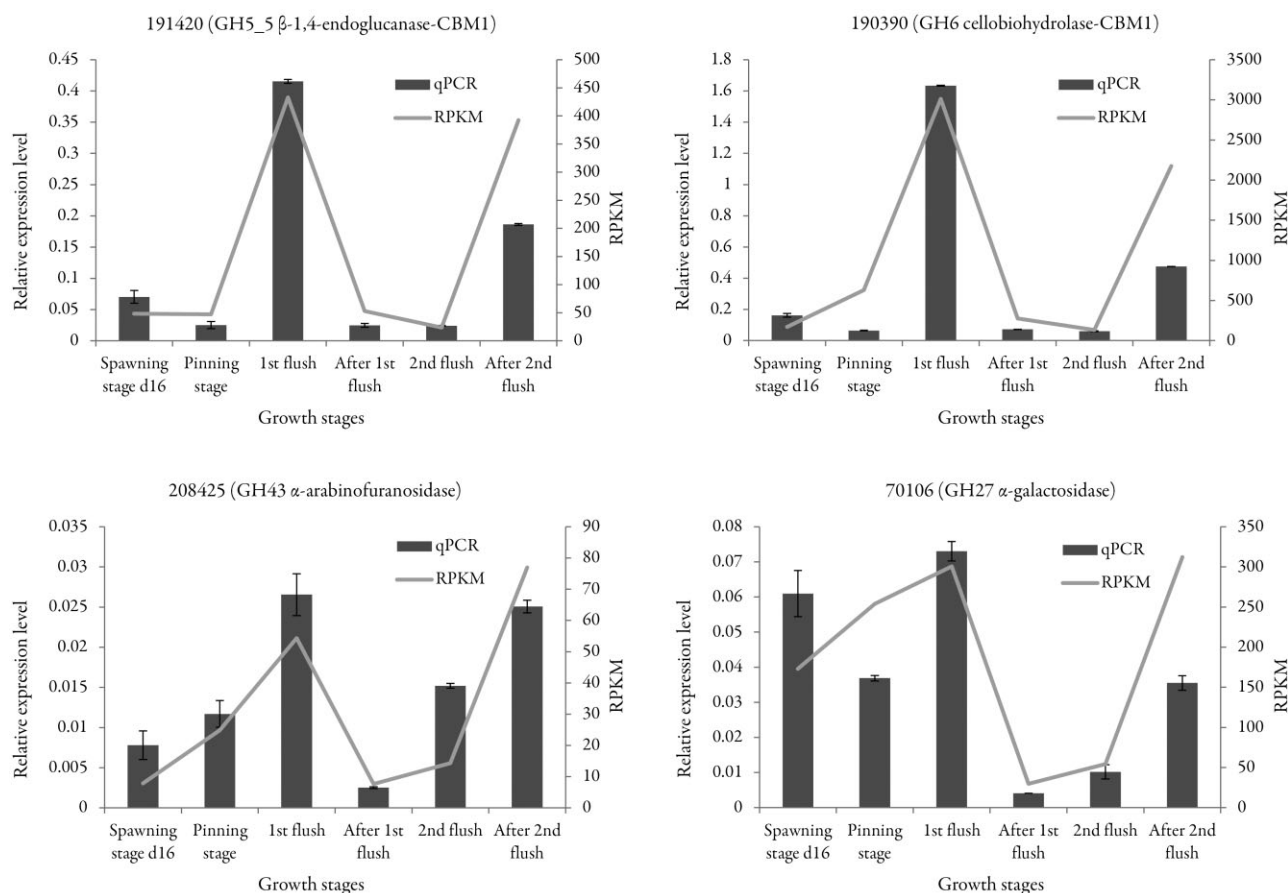


Fig. 2. Expression patterns and validation of RNA-seq analysis by qPCR of four selected genes involved in plant biomass degradation by *A. bisporus* (validation of all 20 genes, see Fig. S1). Columns and bars represent the means and standard errors of qPCR. Lines represent RPKM value.

α -arabinofuranosidase, 4 GH16 β -1,3-endoglucanases, 1 GH12 xyloglucan β -1,4-endoglucanase, 1 GH5_7 endomannanase and 1 CE1, 4 CE4 and 1 CE5 acetylxyylan esterases (Fig. 1).

RNA-seq analysis revealed that genes encoding CAZymes involved in lignin degradation had their greatest transcript abundance of during spawning stage day 16 and lower abundance in all the other growth stages (Fig. 1, Table S1). Highly expressed ligninolytic genes during the cultivation of *A. bisporus* in compost are two AA1_1 laccases, one AA2 manganese peroxidase, two AA3_2 GMC oxidoreductases (glucose-methanol-choline oxidoreductase), four AA5_1 glyoxal oxidases, and one AA6 1,4-benzoquinone reductase.

RNA-seq expression validation by quantitative reverse transcription polymerase chain reaction (qRT-PCR)

In order to validate the expression profiles obtained by the RNA-seq analysis, 20 CAZyme-encoding genes with varying mRNA abundance were tested by qRT-PCR.

Expression trends of the selected genes obtained by qRT-PCR confirmed those obtained with RNA-seq data (Fig. 2, Fig. S1).

Proteomic analysis of secreted proteins

The time between gene expression and production (and if needed secretion) of the corresponding proteins can differ for individual proteins, and therefore proteomes of the various growth stages were also analysed. There were 641 proteins identified with 1% false discovery rate (FDR) for all six growth stages together. A total of 168 (26%) of all secreted proteins were identified as CAZymes (Table S2); 96 (57%) of the identified CAZymes were from GH families, whereas 42 (25%), 17 (10%) and 6 (4%) represent AA, CE and PL families respectively. Protein abundance was approximated by peptide spectrum match (PSM) values and ranked on this basis.

Several cellulose-degrading enzymes were detected in the secretome of *A. bisporus* grown in compost.

Table 1. Selected most abundant proteins secreted by *A. bisporus* during growth in compost.

Gene ID	Putative function	# PSM ^a Spawning stage d16	# PSM ^a pinning stage	# PSM ^a first flush	# PSM ^a After first flush	# PSM ^a second flush	# PSM ^a after second flush
Cellulolytic families							
191420	GH5_5 endoglucanase-CBM1	6.5	15	38	87.5	34	32.5
190390	GH6 cellobiohydrolase-CBM1	9	13.5	56	113	37	51
194521	GH7 cellobiohydrolase-CBM1	21.5	42	161	283.5	122	142.5
219902	GH3 β -glucosidase	6.5	67	78.5	82.5	61.5	72.5
Hemicellulolytic families							
133541	GH10 endoxylanase-CBM1	13.5	23	66	132.5	82	83
196181	GH11 endoxylanase	2.5	10	140	119.5	25	54
70106	GH27 α -galactosidase	16	22.5	69	103	31.5	45
64273	GH31 α -xylosidase	57.5	75	109.5	86	53	67
152299	GH35 β -galactosidase	104	168.5	158.5	178	165	193.5
194576	GH51 α -arabinofuranosidase	81.5	132.5	155.5	132	147.5	167.5
Ligninolytic families							
139148	AA1_1 laccase	545.5	561	108.5	120.5	390.5	293
146228	AA1_1 laccase	293.5	292.5	56	53	176.5	144.5
221245	AA2 manganese peroxidase	48	53.5	44.5	32.5	34	40
193903	AA5_1 glyoxal oxidase	71.5	54.5	65.5	56	44	51.5

a. # PSM Peptide Spectrum Match identified by mass spectrometry RP-nanoLC-MS/MS.

GH6 and GH7 cellobiohydrolases as well as GH5_5 endoglucanases were abundantly produced, demonstrating high correlation with RNA-seq data (Table 1). But unlike the transcriptome profile, which showed a decrease in gene expression at the stage when all the first flush mushrooms were harvested, corresponding CAZymes with cellulolytic activities were still present during that stage (Table 1, Tables S1 and S2). These could be the same proteins that were secreted at the earlier first flush stage when corresponding genes were highly expressed. A drop in protein secretion was observed during the second flush, followed by an increase at the stage when all the second flush mushrooms were harvested, showing a similar trend as was observed for the RNA-seq data.

Also several hemicellulose hydrolysing enzymes were identified and quantified (Table S2). The most abundant secreted proteins were represented by GH10 and GH11 endoxylanases, GH27 α -galactosidase, GH31 α -xylosidase and α -glucosidase, GH35 β -galactosidase and GH51 α -arabinofuranosidase (Table 1). These abundantly produced CAZymes correlate with the RNA-seq analysis of the corresponding genes. A similar pattern of concordance between secretome and transcriptome profiles for hemicellulolytic functions was observed regarding differences between various growth stages of *A. bisporus* as was observed for cellulose degradation.

In addition to cellulases and hemicellulases, we detected a number of ligninolytic enzymes with the AA1_1 laccases being the most abundant (Table 1), which were also the most highly expressed ligninolytic genes in the transcriptome data.

Composition analysis of compost samples

Compost samples of the various growth stages of *A. bisporus* were analysed for cellulose, hemicellulose and lignin contents. Changes in carbohydrate composition of compost samples occurred with mushroom growth. Cellulose and hemicellulose content, based on dry matter, decreased from 14.4 and 10.8 (w/w%) in the compost of the spawning stage day 16, to 8.1 and 5.5 (w/w%), respectively, in the compost of the stage when all the second flush mushrooms were harvested (Table 2, Fig. 1). Lignin composition was measured by analytical pyrolysis and S : G (syringol + vinylsyringol units/guaiacol + vinylguaiacol units) ratio was estimated. In contrast to cellulose and hemicellulose composition, the largest changes in lignin content appeared to happen at the spawning stage day 16 compared with composting stages (Phase I and Phase II of compost) (Jurak, 2015) (Table 2, Fig. 1). No major changes occurred in lignin structure (S : G ratio all in a range of 0.43–0.49, no

Table 2. Composition analysis of compost samples of various growth stages of *A. bisporus*.

Growth stage	Cellulose ^a (w/w%)	Hemicellulose ^{a,b} (w/w%)	Lignin (S/G ratio)
Spawning stage d16	14.4 ± 0.1	10.8 ± 0.1	0.49 ± 0.02
Pinning stage	12.9 ± 1.2	7.7 ± 0.1	0.46 ± 0.01
First flush	10.8 ± 0.6	6.8 ± 0.2	0.43 ± 0.01
After first flush	8.8 ± 0.1	6.3 ± 0.1	0.48 ± 0.06
Second flush	7.6 ± 0.7	5.8 ± 0.3	0.44 ± 0.01
After second flush	8.1 ± 0.2	5.5 ± 0.02	0.46 ± 0.01

a. Presented as anhydro sugars, based on dry matter.

b. Sum of arabinosyl, xylosyl, glucuronic acid.

change) after the spawning stage day 16 until the stage when all second flush mushrooms were harvested (Table 2, Fig. 1).

Central carbohydrate metabolism

Genes associated with central carbohydrate metabolism were identified including glycolysis (27 genes), pentose phosphate pathway (PPP, 14 genes), pentose catabolic pathway (PCP, 4 genes), D-galactose catabolism (12 genes), D-galacturonic acid catabolism (5 genes), L-rhamnose catabolism (2 genes), D-mannose catabolism (4 genes), mannitol metabolism (3 genes), trehalose metabolism (8 genes) and organic acid metabolism (25 genes), and gene expression was analysed at different growth stages of *A. bisporus* (Table S1).

Genes involved in glycolysis, PPP and PCP were expressed during all growth stages of *A. bisporus* (Table S1). Among the highly expressed genes (RPKM values > 300) glyceraldehyde-3-phosphate dehydrogenase (EC 1.2.1.12); enolase (EC 4.2.1.11) and pyruvate kinase (EC 2.7.1.40) encoding genes were detected, which represent key players of glycolysis, as well as transaldolase (EC 2.2.1.2) and 6-phosphogluconate dehydrogenase (EC 1.1.1.44) encoding genes of the PPP (Table S1), indicating hexose utilization by this organism. Only some pentose catabolic genes were highly expressed, namely those encoding L-arabinose (EC 1.1.1.21) and D-xylulose (EC 1.1.1.9) reductases. In contrast, the D-xylulose kinase (EC 2.7.1.17) encoding gene, which is a key enzyme of pentose catabolism, was expressed at much lower level, suggesting that *A. bisporus* favours hexose over pentose utilization.

In most basidiomycetes, mannitol is formed by direct reduction of fructose through mannitol 2-dehydrogenase using either nicotinamide adenine dinucleotide (NAD)⁺ (EC 1.1.67) or nicotinamide adenine dinucleotide phosphate (NADP)⁺ (EC 1.1.1.138) as a cofactor (Hult *et al.*, 1980; Voegelé *et al.*, 2005). A gene encoding mannitol 2-dehydrogenase (EC 1.1.1.138) was identified in the *A. bisporus* genome and has the highest expression at the first flush while this expression decreases (almost five times lower compared with the first flush) at the second flush (Table S1).

Expression of non-CAZy and non-central carbohydrate metabolic genes

To classify the function of the predicted *A. bisporus* genes, the eukaryotic orthologous groups (KOG) (Tatusov *et al.*, 2003), gene ontology (GO) (Ashburner *et al.*, 2000) and Kyoto Encyclopedia of Genes and Genomes (KEGG) (Kanehisa and Goto, 2000) annotations were performed (Table S3). Out of the total 9620 genes, 6545 were asso-

ciated with KOG, 4634 with KEGG and 2983 with GO (component, function and process) respectively.

KOG represented genes were assigned to the four main KOG groups (cellular processes and signalling; information storage and processing; metabolism and poorly characterized) (Table S3). A total of 464 KOG genes were highly expressed reaching an RPKM of greater than 300 during various growth stages of *A. bisporus* in compost. Information storage and processing was found to be the major category from the KOG classifications with approximately 24% (98–113 genes) of the total highly expressed genes during all the growth stages except spawning stage day 16 where only 14% of these genes were significantly expressed (Fig. S2). Most of the upregulated genes in all the growth stages compared to the spawning stage day 16 (10–15%) belong to cellular processes and signalling KOG group (Fig. S2). These include genes encoding guanosinetriphosphate (GTP)-binding protein (gene ID 184342), 20S proteasome subunit (gene ID 193671) and myosin class I (gene ID 182136) (Morin *et al.*, 2012) (Table S3) and have high similarity to genes with the same function from *Laccaria bicolor* (Martin *et al.*, 2008), *Gloeophyllum trabeum* (Floudas *et al.*, 2012), *Coprinopsis cinerea* (Stajich *et al.*, 2010) and *Ceriporiopsis subvermispora* (Fernandez-Fueyo *et al.*, 2012). The majority of the downregulated genes (3–7%) in all the growth stages compared with the spawning stage day 16 represents the category of metabolism (Fig. S2). These include genes involved in secondary metabolism: cytochrome P450 genes (genes ID 120936; 189837) (Morin *et al.*, 2012; Doddapaneni *et al.*, 2013) and a gene encoding sterol C5 desaturase (gene ID 218236) (Morin *et al.*, 2012), which is involved in lipid metabolism (Table S3). These cytochrome P450 genes fall into clans CYP52 (gene ID 120936), which is homologous to the CYP63 family in *Phanerochaete chrysosporium* (Doddapaneni *et al.*, 2005), and to CYP61 (gene ID 189837), which encodes the sterol 22 desaturase in *Saccharomyces cerevisiae* (Skaggs *et al.*, 1996).

Discussion

This study is the first exploration of the transcriptome and proteome of different growth stages of the white button mushroom cultivated in compost, using high throughput RNA-sequencing and mass spectrometry, and is also the most detailed study to date of the progression of plant biomass decay during the life cycle of a basidiomycete fungus. Our integrative analysis of this comprehensive data set demonstrates the capacity of the polysaccharide degradation of *A. bisporus* grown in compost and its ability to utilize this substrate during the cultivation process.

Overall, genes encoding a complete repertoire of cellulolytic and hemicellulolytic (mainly xylanolytic)

activities were highly expressed in compost (Fig. 1), demonstrating a good correlation with the composition of the substrate (Jurak *et al.*, 2014). Furthermore, a high correlation was observed between expression profiles of the RNA-seq and qRT-PCR data (Fig. 2, Fig. S1).

Our results indicate that when *A. bisporus* was cultivated in compost in an indoor, controlled commercial environment, the expression pattern of CAZyme-encoding genes and corresponding extracellular protein production changed over time during its life cycle. Figure 1 shows an overview of the major expression changes concerning plant polysaccharide degradation. Interestingly, the transcriptome analysis revealed large differences in expression of genes encoding cellulases and hemicellulases between the first flush when these genes were highly expressed and the second flush when low expression was observed. Such a difference in gene expression might in part explain the difference in yield between two different flushes and could point to a non-synchronicity in gene expression requirement during the second flush under these cultivation conditions. During the first flush, yield of the mushrooms was 21 kg m⁻², whereas the second flush only yielded 8.5 kg m⁻². It is possible that an earlier stimulation of gene expression during the second flush could potentially lead to higher mushroom production.

Ligninolytic genes showed a different expression pattern than the (hemi-) cellulolytic genes. These genes were highly expressed during the spawning stage day 16 and had low expression during all the other stages (Fig. 1, Table S1). This expression pattern corresponds with analytical pyrolysis which showed that the lignin fraction of compost remained practically constant after spawning stage and until the entire second flush was harvested (Fig. 1). This could indicate that lignin is not modified after the spawning stage.

Finally, secretome analysis supported the important role for many genes involved in plant biomass degradation, particularly those associated with high transcript levels. However, the correlation between gene expression and protein production changed during the life cycle of *A. bisporus*. Variation between transcriptome and proteome was observed after the entire first flush was harvested when gene expression levels decreased while enzymes were still highly abundant. Most likely, the proteins were secreted at the first flush stage and remained active in compost. Lack of correlation between transcriptomics and proteomics data can be due to various factors such as different levels of regulation, stability of mRNA, rate of mRNA transcription and protein translation as well as protein stability and the biochemical diversity of proteins (Fournier *et al.*, 2010; Vogel *et al.*, 2011; Vogel and Marcotte, 2012). This could explain the variation in the correlation between the secretion level of individual proteins and the expression level of their corresponding genes.

Extensive studies of transcriptome and secretome of various wood-decaying basidiomycete fungi involved time-dependent degradation or modification of lignocellulosic substrates. For example, wood decay by the white rot fungus *Phanerochaete carmosa* revealed high expression levels of ligninolytic genes (lignin and manganese peroxidases) at early stages of cultivation followed by high expression levels of (hemi-)cellulolytic genes (cellobiohydrolase, xylanase, mannanase, acetyl xylan and glucuronoyl esterases) at later stages of cultivation (MacDonald and Master, 2012). Sequential production of lignocellulose-degrading enzymes was also detected during cultivation of another white rot basidiomycete *C. subvermispota*, which showed early production of ligninolytic enzymes (laccase, manganese peroxidase, aryl alcohol oxidase) followed by production of cellulose and hemicellulose main chains cleaving endo-acting enzymes (GH10 endoxylanase, GH5_5 endoglucanase and GH7 cellobiohydrolase) and, in the end of cultivation, a variety of cellulose-degrading enzymes along with GH10 endoxylanase were dominant (Hori *et al.*, 2014). The similarity in genome composition of *A. bisporus* with white rot fungi (Morin *et al.*, 2012) is also supported by the expression profile obtained in our study.

In addition to capabilities of *A. bisporus* to degrade plant polysaccharides present in compost during its life cycle, central carbon metabolism including all major pathways as well as storage carbohydrate metabolism were studied at different growth stages of white button mushroom. Carbon catabolic genes were expressed during the entire cultivation process of *A. bisporus* in compost starting from spawning stage day 16 until all the second flush mushrooms were harvested. This active metabolism throughout its life cycle indicates that *A. bisporus* does not have dormant phases in this method of cultivation. Genes encoding enzymes with essential metabolic role from glycolysis and PPP were highly expressed compared with PCP, indicating that *A. bisporus* prefers hexoses over pentoses.

Regarding organic acid metabolism, genes encoding glyoxylate (GLOX) cycle key enzymes (isocitrate lyase and malate synthase) (Munir *et al.*, 2001) were significantly expressed, whereas genes encoding essential enzymes of TCA (isocitrate dehydrogenase, 2-oxoglutarate dehydrogenase and citrate synthase) (Matsuzaki *et al.*, 2008; Kubicek *et al.*, 2011) had low expression (Table S1). This could indicate a higher flux in the GLOX cycle compared with TCA. It has been reported that basidiomycetes have a bicycle TCA/GLOX system, and malate can be shuttled from one cycle to the other and be oxidized by malate dehydrogenase to oxaloacetate, which further can be converted to oxalate (Munir *et al.*, 2001). The high expression of genes

Table 3. Growth stages of *A. bisporus* mycelium colonized compost used in this study.

Compost sample	Description	Days after spawns were introduced into Phase II compost
Spawning stage d16	Compost at the end of the spawning stage	16
Pinning stage	Compost when pinning has clearly started and the first pinheads were visible	30
First flush	Compost of the first flush, pinheads have become harvestable mushrooms	39
After first flush	Compost after all first flush was harvested	40
Second flush	Compost of the second flush, pinheads have become harvestable mushrooms	45
After second flush	Compost after all second flush was harvested	48

encoding malate dehydrogenase, isocitrate lyase and malate synthase during growth of *A. bisporus* in compost suggests a need for the production of oxalate under these conditions (Table S1). It has been demonstrated that oxalic acid plays a crucial role in initial lignocellulose degradation before enzymatic hydrolysis (Hastrup *et al.*, 2011). Oxalic acid typically accumulates in cultures of brown rot fungi, whereas it is detected in lower amounts in white rot fungi (Dutton *et al.*, 1993; Mäkelä *et al.*, 2002; Hastруп *et al.*, 2012). Moreover, metabolic change at the transition step from vegetative growth to fruiting body formation of brown rot fungus *Fomitopsis palustris* in the GLOX and TCA cycles was observed. Oxalate biosynthesis played an important role in vegetative growth, whereas glutamate synthesis played a major role in fruiting body formation (Yoon *et al.*, 2002). However, no significant correlation between growth stages of *A. bisporus* and GLOX/TCA cycles were found in our data. Further research is needed to better understand the role of GLOX/TCA cycles in *A. bisporus* throughout its life cycle.

Another interesting feature that was observed refers to mannitol metabolism. It has been shown that mannitol acts as an osmoregulatory compound promoting a flow of water from compost to the fruiting body to maintain turgor and fruiting body development in *A. bisporus* (Kalberer, 1990; Stoop and Mooibroek, 1998). Additionally, it has been demonstrated that genes involved in mannitol pathway were significantly lower in fruiting bodies than in compost, which indicated synthesis of mannitol in the vegetative mycelium and its transport to the fruiting body (Patyshakuliyeva *et al.*, 2013). Mannitol 2-dehydrogenase is a key enzyme for mannitol production in most basidiomycetes (Hult *et al.*, 1980; Voegelé *et al.*, 2005). In this study, we observed that the gene encoding this enzyme had the highest expression at the first flush, whereas at the second flush, the expression level of this gene decreased (Table S1). Referring to the importance of mannitol for fruiting body development, low expression of mannitol 2-dehydrogenase gene at the second flush may correspond with lower number of mushrooms harvested at the second flush compared with the first flush. Together with the lower expression of (hemi-)cellulolytic genes in the second flush, this indicates significant differ-

ences in the physiology of *A. bisporus* during production of the first and second flush mushrooms.

In conclusion, our integrative analysis of various growth stages of *A. bisporus* cultivated in compost in a controlled environment demonstrates changes in plant biomass degradation throughout its life cycle. Most notable differences in gene expression were detected between first and second flushes, which involved cellulolytic and hemicellulolytic genes as well as the mannitol 2-dehydrogenase encoding gene. This observation could explain the loss in the number of mushrooms during second flush.

Experimental procedures

Strain and sample collection

Agaricus bisporus commercial heterokaryon strain A15 (Sylvan, USA) was used in this study. The sequenced H97 together with H39 are homokaryons and parental strains of the commercial strain U1. Commercial mushroom strain A15 is a clone of U1 and developed by clonal vegetative propagation, or quasi-clones derived from spores that retain the great majority of the parental genotype (Kerrigan *et al.*, 1993). A15 shares a single basic genotype with U1. Phases I and II mushroom compost, which is based on wheat straw, horse and chicken manure, gypsum and water, were prepared according to commercial practice at CNC-C4C (Milsbeek, the Netherlands). Phase II compost was inoculated with *A. bisporus* spawns (Sylvan) and incubated at 25°C for 16 days. Fully colonized compost was covered with casing layer (peat and lime) according to established commercial practice and incubated until first and second flushes of mushrooms were developed and harvested.

Mycelium colonized compost samples were collected at the different growth stages of *A. bisporus* (Table 3). Compost samples were taken in duplicate for each growth stage. All samples were immediately frozen and stored at -20°C until being processed for transcriptome, secretome, carbohydrate composition analysis and pyrolysis.

RNA extraction, cDNA library preparation and RNA-seq

Total RNA was isolated from the collected compost samples using a CsCl gradient centrifugation method (Patyshakuliyeva *et al.*, 2014). RNA integrity and quantity were checked with the RNA6000 Nano Assay using the Agilent 2100 Bioanalyzer (Agilent Technologies, Santa Clara,

CA, USA). cDNA library preparation and sequencing reactions were conducted in the BGI Tech Solutions (Hong Kong). Illumina library preparation, clustering and sequencing reagents were used throughout the process following the manufacturer's recommendations (<http://illumina.com>). Briefly, mRNA was purified using poly-T oligonucleotide-attached magnetic beads and then fragmented. The first and second strands cDNA were synthesized and end repaired. Adaptors were ligated after adenylation at the 3' end. After gel purification, cDNA templates were enriched by PCR. cDNA libraries were validated using the Agilent 2100 Bioanalyzer (Agilent Technologies) and quantified by qPCR. Single-read samples were sequenced using Illumina HiSeq™ 2000 platform (<http://illumina.com>). In average 51 bp sequenced reads were constituted, producing approximately 450MB raw yields for each sample.

RNA-seq data analysis and functional annotation

Raw reads were produced from the original image data by base calling. After data filtering, the adaptor sequences, highly 'N' containing reads (> 10% of unknown bases) and low quality reads (more than 50% bases with quality value of < 5%) were removed. After data filtering, in average, ~ 95% clean reads remained in each sample; the average amount of clean reads was 11.84 M. Clean reads were then mapped to the genome of *Agaricus bisporus* var *bisporus* (H97) v2.0 (Morin *et al.*, 2012) using SOAPALIGNER/SOAP2 (Li *et al.*, 2009). No more than two mismatches were allowed in the alignment. In average, 76.44% total mapped reads to the genome was achieved. The gene expression level was calculated by using RPKM method (Mortazavi *et al.*, 2008). Genes with expression value higher than 300 were considered highly expressed (approximately top 5%, Table S4) and differential expression was identified by CyberT bayesianANOVA algorithm (Kayala and Baldi, 2012) with a cut-off value of fold change > 1.5 and *P*-value (corrected by multiple tests) < 0.05. The RNA-seq data have been submitted to Gene Expression Omnibus (GEO) (Edgar *et al.*, 2002) with accession number: GSE65800.

Gene sequences were aligned to NCBI non-redundant (Nr) and InterPro database (Mitchell *et al.*, 2015) for functional annotations using BLASTX (Mount, 2007) with a cut-off value of 1E-20. Information on GO (Ashburner *et al.*, 2000), COG (Tatusov *et al.*, 2003) and KEGG (Kanehisa and Goto, 2000) were downloaded from Joint Genome Institute (http://genome.jgi-psf.org/Agabi_varbisH97_2/) using default settings. Proteins with putative signal peptide were predicted by SIGNALP 4.0 (Petersen *et al.*, 2011). The annotations were then mapped to the expressed genes accordingly.

qRT-PCR validation

RNA samples for RNA-seq experiments were also used for qRT-PCR validation of genes with varying transcript abundance. Briefly, 2 µg RNA was converted into cDNA in 20 µl of reaction (ThermoScript™ RT-PCR System, Invitrogen, Carlsbad, CA, USA) according to the instructions of the manufacturer.

The sequences of all primers for qRT-PCR analysis were designed using the PRIMER EXPRESS 3.0 software (Applied

Biosystems, Foster City, CA, USA). The primers were tested to determine the optimal primer concentrations and efficiency. Combinations of the 50 nM, 300 nM and 900 nM (final concentration) per primer pair were checked, and based on the dissociation curve, the optimal primer concentration per primer pair was set. The primer sequences and optimal concentrations of the tested genes and the reference gene are listed in Table S5.

qRT-PCR was performed using an ABI 7500 fast real-time PCR system (Applied Biosystems). The 20 µl reactions consisted of 2 µl forward and reverse primers at optimal concentration, 20 ng cDNA sample, 10 µl ABI Fast SYBR Master Mix (Applied Biosystems) and water to a final volume of 20 µl. The cycling parameters were 95°C for 20 s, followed by 40 cycles of 95°C for 3 s and 60°C for 30 s. A dissociation curve was generated to verify that a single product was amplified. Transcript levels were normalized against the *gpd* gene (glyceraldehyde-3-phosphate dehydrogenase, *A. bisporus* genome Gene ID: 138631) expression and quantified according to the formula $2^{-(Ct_{gene} - Ct_{gpd})}$ (Livak and Schmittgen, 2001). Control reactions included water only and RNA (i.e. not converted to cDNA to detect residual DNA in the sample). Two biological and three technical replicates were analysed.

Secretome extraction

For secretomic analysis, collected mycelium grown compost (10 g) samples (Table 3) were mixed with distilled water (100 ml) in 250 cm³ Erlenmeyer flasks. All the flasks were placed in an incubator shaker at 200 r.p.m. for 1 h at 4°C. The samples were then centrifuged at 10 000 r.p.m. for 15 min and the supernatant was concentrated 4× using a vacuum concentrator Speedvac (Savant Instruments, Farmingdale, NY, USA).

Protein preparation and analysis by mass spectrometry

Protein separation and digestion. The 30 µl of each of the samples were run on a 12% Bis-Tris 1D SDS-PAGE gel (Bio-Rad) for 2–3 cm and stained with colloidal coomassie dye G-250 (Gel Code Blue Stain Reagent, Thermo Scientific, Bremen, Germany). The lane was cut into two bands, which were treated with 6.5 mM dithiothreitol for 1 h at 60°C for reduction and 54 mM iodoacetamide for 30 min for alkylation. The proteins were digested overnight with trypsin (Promega) at 37°C. The peptides were extracted with 100% acetonitrile (ACN) and dried in a vacuum concentrator (Thermo Scientific).

Mass spectrometry: ReversePhase-nanoLC-MS/MS. Samples were resuspended in 10% formic acid (FA)/5% dimethylsulphoxide, and 30% of the sample was analysed using a Proxeon Easy-nLC100 (Thermo Scientific) connected to an Orbitrap Q-Exactive mass spectrometer. Samples were first trapped (Dr Maisch Reprosil C18, 3 µm, 2 cm × 100 µm) before being separated on an analytical column (Agilent Poroshell EC-C18, 2.7 µm, 40 cm × 50 µm), using a gradient of 60 min at a column flow of 150 nl min⁻¹. Trapping was performed at 8 µl min⁻¹ for 10 min in solvent A (0.1 M acetic

acid in water) and the gradient was as follows: 7–30% solvent B (0.1 M acetic acid in ACN) in 31 min, 30–100% in 3 min, 100% solvent B for 5 min, and 7% solvent B for 13 min. Nanospray was performed at 1.7 kV using a fused silica capillary that was pulled in-house and coated with gold (o.d. 360 µm; i.d. 20 µm; tip i.d. 10 µm). The mass spectrometers were used in a data-dependent mode, which automatically switched between MS and MS/MS. Full scan MS spectra from m/z 350–1500 were acquired at a resolution of 35,000 at m/z 400 after the accumulation to a target value of 3E6. Up to 10 most intense precursor ions were selected for fragmentation. Higher-energy collisional dissociation fragmentation was performed at normalized collision energy of 25% after the accumulation to a target value of 5e4. MS2 was acquired at a resolution of 17,500 and dynamic exclusion was enabled (exclusion size list 500, exclusion duration 10 s).

Data analysis. Raw files were processed using PROTEOME DISCOVERER 1.3 (version 1.3.0.339, Thermo Scientific). Database search was performed using the genome of *A. bisporus* var. *bisporus* (H97) v2.0 (Morin *et al.*, 2012) and Mascot (version 2.4.1, Matrix Science, UK) as the search engine. Carbamidomethylation of cysteines was set as a fixed modification and oxidation of methionine was set as a variable modification. Trypsin was specified as enzyme and up to two miss cleavages were allowed. Data filtering was performed using percolator, resulting in 1% FDR. Additional filters were search engine rank 1 peptides and Mascot ion score > 20. Raw files corresponding to one sample were merged into one result file. The mass spectrometry proteomics data have been deposited to the ProteomeXchange Consortium (Vizcaino *et al.*, 2014) via the Proteomics Identifications Database (PRIDE) (Martens *et al.*, 2005) partner repository with the dataset identifier PXD001817.

Pyrolysis and carbohydrate composition analysis of compost

Neutral carbohydrate content and composition were determined in duplicates, as described by Jurak and colleagues (2014). Lignin composition was determined by analytical pyrolysis-GC-MS (Py-GC/MS) method (Jurak, 2015).

Acknowledgements

AP and EJ were supported by grants from the Dutch Technology Foundation STW (Applied Science division of NWO) and the Technology Program of the Ministry of Economic Affairs UGC 11108. MZ was supported by a grant from the Netherlands Organisation for Scientific Research (NWO) and the Netherlands Genomics Initiative 93511035 to RPDV. The data analysis was partially carried out on the Dutch national e-infrastructure with the support of SURF Foundation (e-infra130078). We kindly acknowledge the project 'Proteins at Work', financed by the Netherlands Organisation for Scientific Research (NWO) as part of the National Roadmap Large-Scale Research Facilities of the Netherlands (project number 184.032.201). The authors thank Wim Arts and Geert Weijers for supplying compost samples.

References

- Ashburner, M., Ball, C.A., Blake, J.A., Botstein, D., Butler, H., Cherry, J.M., *et al.* (2000) Gene ontology: tool for the unification of biology. The Gene Ontology Consortium. *Nat Genet* **25**: 25–29.
- Chang, S.T., and Miles, P.G. (1989) *Edible Mushrooms and Their Cultivation*. Boca Raton, FL, USA: CRC Press.
- Doddapaneni, H., Subramanian, V., and Yadav, J.S. (2005) Physiological regulation, xenobiotic induction, and heterologous expression of P450 monooxygenase gene *pc-3* (CYP63A3), a new member of the CYP63 gene cluster in the white-rot fungus *Phanerochaete chrysosporium*. *Curr Microbiol* **50**: 292–298.S
- Doddapaneni, H., Subramanian, V., Fu, B., and Cullen, D. (2013) A comparative genomic analysis of the oxidative enzymes potentially involved in lignin degradation by *Agaricus bisporus*. *Fungal Genet Biol* **55**: 22–31.
- Dutton, M., Evans, C., Atkey, P., and Wood, D. (1993) Oxalate production by basidiomycetes, including the white-rot species *Coriolus versicolor* and *Phanerochaete chrysosporium*. *Appl Microbiol Biotechnol* **39**: 5–10.
- Edgar, R., Domrachev, M., and Lash, A.E. (2002) Gene expression Omnibus: NCBI gene expression and hybridization array data repository. *Nucleic Acids Res* **30**: 207–210.
- Fernandez-Fueyo, E., Ruiz-Duenas, F.J., Ferreira, P., Floudas, D., Hibbett, D.S., Canessa, P., *et al.* (2012) Comparative genomics of *Ceriporiopsis subvermisporea* and *Phanerochaete chrysosporium* provide insight into selective ligninolysis. *Proc Natl Acad Sci USA* **109**: 5458–5463.
- Floudas, D., Binder, M., Riley, R., Barry, K., Blanchette, R.A., Henrissat, B., *et al.* (2012) The Paleozoic origin of enzymatic lignin decomposition reconstructed from 31 fungal genomes. *Science* **336**: 1715–1719.
- Fournier, M.L., Paulson, A., Pavelka, N., Mosley, A.L., Gaudenz, K., Bradford, W.D., *et al.* (2010) Delayed correlation of mRNA and protein expression in rapamycin-treated cells and a role for Ggc1 in cellular sensitivity to rapamycin. *Mol Cell Proteomics* **9**: 271–284.
- Gerrits, J. (1969) Organic compost constituents and water utilized by the cultivated mushroom during spawn run and cropping. *Mushroom Sci* **7**: 1–126.
- Gerrits, J., Bels-Koning, H., and Muller, F. (1967) Changes in compost constituents during composting, pasteurization and cropping. *Mushroom Sci* **6**: 225–243.
- Gerrits, J.P.G. (1988) Nutrition and compost. In *The Cultivation of Mushrooms*. Van Griensven, L.J.L.D. (ed.). Horst, The Netherlands: Springer Netherlands, pp. 29–72.
- Hastrup, A.C.S., Howell, C., Jensen, B., and Green Iii, F. (2011) Non-enzymatic depolymerization of cotton cellulose by fungal mimicking metabolites. *Int Biodet Biodegr* **65**: 553–559.
- Hastrup, A.C.S., Green Iii, F., Lebow, P.K., and Jensen, B. (2012) Enzymatic oxalic acid regulation correlated with wood degradation in four brown-rot fungi. *Int Biodeter Biodegr* **75**: 109–114.
- Hilden, K., Makela, M.R., Lankinen, P., and Lundell, T. (2013) *Agaricus bisporus* and related *Agaricus* species on lignocellulose: production of manganese peroxidase and multicopper oxidases. *Fungal Genet Biol* **55**: 32–41.

- Hori, C., Gaskell, J., Igarashi, K., Kersten, P., Mozuch, M., Samejima, M., and Cullen, D. (2014) Temporal alterations in the secretome of the selective ligninolytic fungus *Ceriporiopsis subvermispora* during growth on aspen wood reveal this organism's strategy for degrading lignocellulose. *Appl Environ Microbiol* **80**: 2062–2070.
- Hult, K., Veide, A., and Gatenbeck, S. (1980) The distribution of the NADPH-regenerating mannitol cycle among fungal species. *Arch Microbiol* **128**: 253–255.
- Iiyama, K., Stone, B.A., and Macauley, B.J. (1994) Compositional changes in compost during composting and growth of *Agaricus bisporus*. *Appl Environ Microbiol* **60**: 1538–1546.
- Jurak, E. (2015) How mushrooms feed on compost: conversion of carbohydrates and lignin in industrial wheat straw based compost enabling the growth of *Agaricus bisporus*. PhD Thesis, Wageningen, The Netherlands: Wageningen University.
- Jurak, E., Kabel, M.A., and Gruppen, H. (2014) Carbohydrate composition of compost during composting and mycelium growth of *Agaricus bisporus*. *Carbohydr Poly* **101**: 281–288.
- Kalberer, P.P. (1990) Influence of the water potential of the casing soil on crop yield and on dry-matter content, osmotic potential and mannitol content of the fruit bodies of *Agaricus bisporus*. *J Horticul Sci* **65**: 573–581.
- Kanehisa, M., and Goto, S. (2000) KEGG: Kyoto Encyclopedia of Genes and Genomes. *Nucleic Acids Res* **28**: 27–30.
- Kayala, M.A., and Baldi, P. (2012) Cyber-T web server: differential analysis of high-throughput data. *Nucleic Acids Res* **40**: 553–559.
- Kerrigan, R.W., Royer, J.C., Baller, L.M., Kohli, Y., Horgen, P.A., and Anderson, J.B. (1993) Meiotic behavior and linkage relationships in the secondarily homothallic fungus *Agaricus bisporus*. *Genetics* **133**: 225–236.
- Kubicek, C., Punt, P., and Visser, J. (2011) Production of organic acids by filamentous fungi. In *Industrial Applications*. Hofrichter, M. (ed.). Berlin, Germany: Springer, pp. 215–234.
- Li, R., Yu, C., Li, Y., Lam, T.W., Yiu, S.M., Kristiansen, K., and Wang, J. (2009) SOAP2: an improved ultrafast tool for short read alignment. *Bioinformatics* **25**: 1966–1967.
- Livak, K.J., and Schmittgen, T.D. (2001) Analysis of relative gene expression data using real-time quantitative PCR and the $2^{-\Delta\Delta CT}$ method. *Methods* **25**: 402–408.
- Lombard, V., Golaconda Ramulu, H., Drula, E., Coutinho, P.M., and Henrissat, B. (2014) The carbohydrate-active enzymes database (CAZy) in 2013. *Nucleic Acids Res* **42**: 490–495.
- MacDonald, J., and Master, E.R. (2012) Time-dependent profiles of transcripts encoding lignocellulose-modifying enzymes of the white rot fungus *Phanerochaete carmosa* grown on multiple wood substrates. *Appl Environ Microbiol* **78**: 1596–1600.
- Martens, L., Hermjakob, H., Jones, P., Adamski, M., Taylor, C., States, D., et al. (2005) PRIDE: the proteomics identifications database. *Proteomics* **5**: 3537–3545.
- Martin, F., Aerts, A., Ahren, D., Brun, A., Danchin, E.G., Duchaussoy, F., et al. (2008) The genome of *Laccaria bicolor* provides insights into mycorrhizal symbiosis. *Nature* **452**: 88–92.
- Matsuzaki, F., Shimizu, M., and Wariishi, H. (2008) Proteomic and metabolomic analyses of the white-rot fungus *Phanerochaete chrysosporium* exposed to exogenous benzoic acid. *J Proteome Res* **7**: 2342–2350.
- Mäkelä, M., Galkin, S., Hatakka, A., and Lundell, T. (2002) Production of organic acids and oxalate decarboxylase in lignin-degrading white rot fungi. *Enzyme Microb Technol* **30**: 542–549.
- Mitchell, A., Chang, H.Y., Daugherty, L., Fraser, M., Hunter, S., Lopez, R., et al. (2015) The InterPro protein families database: the classification resource after 15 years. *Nucleic Acids Res* **43**: 213–221.
- Morin, E., Kohler, A., Baker, A.R., Foulongne-Oriol, M., Lombard, V., Nagy, L.G., et al. (2012) Genome sequence of the button mushroom *Agaricus bisporus* reveals mechanisms governing adaptation to a humic-rich ecological niche. *Proc Natl Acad Sci USA* **109**: 17501–17506.
- Mortazavi, A., Williams, B.A., McCue, K., Schaeffer, L., and Wold, B. (2008) Mapping and quantifying mammalian transcriptomes by RNA-Seq. *Nat Methods* **5**: 621–628.
- Mount, D.W. (2007) Using the basic local alignment search tool (BLAST). *CSH Protoc* **2007**: 17.
- Munir, E., Yoon, J.J., Tokimatsu, T., Hattori, T., and Shimada, M. (2001) A physiological role for oxalic acid biosynthesis in the wood-rotting basidiomycete *Fomitopsis palustris*. *Proc Natl Acad Sci USA* **98**: 11126–11130.
- Patyshakuliyeva, A., Jurak, E., Kohler, A., Baker, A., Battaglia, E., de Bruijn, W., et al. (2013) Carbohydrate utilization and metabolism is highly differentiated in *Agaricus bisporus*. *BMC Genomics* **14**: 663.
- Patyshakuliyeva, A., Mäkelä, M.R., Sietiö, O.M., de Vries, R.P., and Hildén, K.S. (2014) An improved and reproducible protocol for the extraction of high quality fungal RNA from plant biomass substrates. *Fungal Genet Biol* **72**: 201–206.
- Petersen, T.N., Brunak, S., von Heijne, G., and Nielsen, H. (2011) SignalP 4.0: discriminating signal peptides from transmembrane regions. *Nat Methods* **8**: 785–786.
- Skaggs, B.A., Alexander, J.F., Pierson, C.A., Schweitzer, K.S., Chun, K.T., Koegel, C., et al. (1996) Cloning and characterization of the *Saccharomyces cerevisiae* C-22 sterol desaturase gene, encoding a second cytochrome P-450 involved in ergosterol biosynthesis. *Gene* **169**: 105–109.
- Stajich, J.E., Wilke, S.K., Ahren, D., Au, C.H., Birren, B.W., Borodovsky, M., et al. (2010) Insights into evolution of multicellular fungi from the assembled chromosomes of the mushroom *Coprinopsis cinerea* (*Coprinus cinereus*). *Proc Natl Acad Sci USA* **107**: 11889–11894.
- Stoop, J.M., and Mooibroek, H. (1998) Cloning and characterization of NADP-mannitol dehydrogenase cDNA from the button mushroom, *Agaricus bisporus*, and its expression in response to NaCl stress. *Appl Environ Microbiol* **64**: 4689–4696.
- Tatusov, R.L., Fedorova, N.D., Jackson, J.D., Jacobs, A.R., Kiryutin, B., Koonin, E.V., et al. (2003) The COG database: an updated version includes eukaryotes. *BMC Bioinformatics* **4**: 41.

- Van Griensven, L. (1988) *The Cultivation of Mushrooms*. Rustington, Sussex, UK: Darlington Mushroom Laboratories.
- Vizcaino, J.A., Deutsch, E.W., Wang, R., Csordas, A., Reisinger, F., Rios, D., *et al.* (2014) ProteomeXchange provides globally coordinated proteomics data submission and dissemination. *Nat Biotechnol* **32**: 223–226.
- Voegele, R.T., Hahn, M., Lohaus, G., Link, T., Heiser, I., and Mendgen, K. (2005) Possible roles for mannitol and mannitol dehydrogenase in the biotrophic plant pathogen *Uromyces fabae*. *Plant Physiol* **137**: 190–198.
- Vogel, C., and Marcotte, E.M. (2012) Insights into the regulation of protein abundance from proteomic and transcriptomic analyses. *Nat Rev Genet* **13**: 227–232.
- Vogel, C., Silva, G.M., and Marcotte, E.M. (2011) Protein expression regulation under oxidative stress. *Mol Cell Proteomics* **10**: M111 009217.
- Wood, D., Thurston, C., and Griensven, L. (1991) Progress in the molecular analysis of *Agaricus* enzymes. In *Genetics and Breeding of Agaricus: Proceedings of the First International Seminar on Mushroom Science, Mushroom Experimental Station, 14–17 May 1991*. van Griensven, L. (ed.). Horst, The Netherlands: Pudoc, pp. 81–86.
- Yague, E., Mehak-Zunic, M., Morgan, L., Wood, D.A., and Thurston, C.F. (1997) Expression of Cel2 and Cel4, two proteins from *Agaricus bisporus* with similarity to fungal cellobiohydrolase I and beta-mannanase, respectively, is regulated by the carbon source. *Microbiology* **143**: 239–244.
- Yoon, J.J., Hattori, T., and Shimada, M. (2002) A metabolic role of the glyoxylate and tricarboxylic acid cycles for development of the copper-tolerant brown-rot fungus *Fomitopsis palustris*. *FEMS Microbiol Lett* **217**: 9–14.

Supporting information

Additional Supporting Information may be found in the online version of this article at the publisher's web-site:

Fig. S1. Expression patterns and validation of RNA seq analysis by qPCR of twenty selected genes involved in plant

biomass degradation by *A. bisporus*. Columns and bars represent the means and standard errors of qPCR. Lines represent RPKM value.

Fig. S2. Percentage distribution of KOG functional classification related genes. Distribution of the genes which are highly expressed (RPKM > 300) during the growth of *A. bisporus* in compost (A); are differentially expressed (all the growth stages compared to spawning stage day 16): upregulated (B) and downregulated (C).

Table S1. Expression of known genes involved in central metabolism (sheet 1) and CAZymes (sheet 2) of *A. bisporus*. The expression higher than 300 is considered highly expressed and marked red. The genes with expression lower than 15 (lowest 40%) are considered low expressed and marked green. The comparisons between different conditions are listed behind, the cutoff for differential expression is fold change > 1.5 (cells marked red if upregulated and green if downregulated) and *P*-value < 0.05 (cells marked yellow).

Table S2. *A. bisporus* proteins secreted during its growth in compost.

Table S3. Expression of all expressed genes (sheet 1) with functional annotations; top 5% highly expressed genes (expression value higher than 300, sheet 2) and the genes that are significantly differentiated on at least one condition comparing to the expression at the spawning stage (sheet 3). Gene that have fold change > 1.5 are marked red if upregulated and green if downregulated and *P*-value < 0.05 are marked yellow in the comparison panels, highly expressed genes with expression value higher than 300 are marked red and the lowly (< 15) expressed ones are marked green in the expression panels. Genes are grouped by their KOG groups based on their (putative) functions.

Table S4. Statistical summary of RNA abundance on all sequenced samples. The expression value of top 5% (300) was used as the cutoff for significantly expressed genes and 15 (40%) was used for the cutoff of lowly expressed genes.

Table S5. Primers used for qRT-PCR.

File 1. Supporting data for reference gene selection.